REFERENCES

[1] J. E. Walsh, T. C. Marshall, M. R. Mross, and S. P. Schlesinger, "Relativistic electron-beam-generated coherent submillimeter wavelength Cerenkov radiation," *IEEE Trans. Microwave Theory Tech.*, vol. MTT-25, pp. 561–563, June 1977.

[2] J. E. Walsh, "Cerenkov and Cerenkov-Raman radiation sources," in *Free-Electron Generators of Coherent Radiation*, S. F. Jacobs, H. S. Pilloff, M. Sargent III, M. O. Scully, and R. Spitzer, Eds. Reading, MA: Addison-Wesley, 1980, pp. 255–300.

[3] T. C. Marshall, S. P. Schlesinger, and D. B. McDermott, "The free-electron laser: A high-power submillimeter radiation source," in *Advances in Electronics and Electron Physics*, vol. 53, L. Marton and C. Marton, Eds. New York: Academic Press, 1980, pp. 47–84.

[4] R. S. Symons and H. R. Jory, "Cyclotron resonance devices," in *Advances in Electronics and Electron Physics*, vol. 55, edited by L. Marton and C. Marton, Eds. New York: Academic Press, 1981, pp. 1–75.

[5] R. E. Collin, *Foundations for Microwave Engineering*. New York: McGraw-Hill, 1966, pp. 439–446.

[6] P. F. Ottinger and J. Guillory, "Beam-plasma interactions in a filled waveguide immersed in applied axial magnetic field," *Phys. Fluids*, vol. 22, pp. 466–475, Mar. 1979.

[7] A. W. Trivelpiece and R. W. Gould, "Space charge waves in cylindrical plasma columns," *J. Appl. Phys.*, vol. 30, pp. 1784–1793, 1959.

[8] R. W. Gould and A. W. Trivelpiece, "A new mode of wave propagation on electron beams," in *Proc. Symp. Electronic Waveguides* edited by J. Fox, Ed. New York: Polytechnic Press, 1958, pp. 215–228.

[9] A. W. Trivelpiece, *Slow-Wave Propagation in Plasma Waveguides*. San Francisco CA: San Francisco Press, 1967, pp. 8–19.

[10] W. P. Allis, S. J. Buchsbaum, and A. Bers, *Waves in Anisotropic Plasmas*. Cambridge, MA: M.I.T. Press, 1963, pp. 121–126.

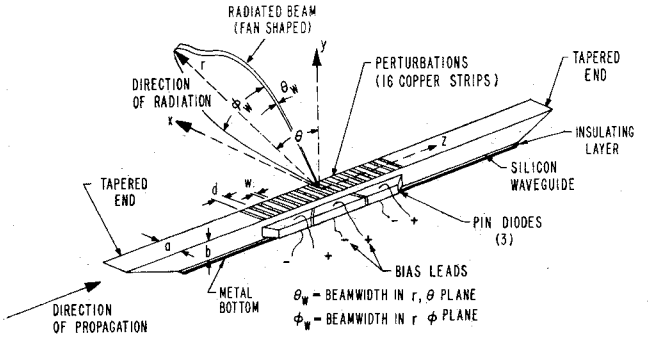

Fig. 1. Line scanning antenna, configuration.

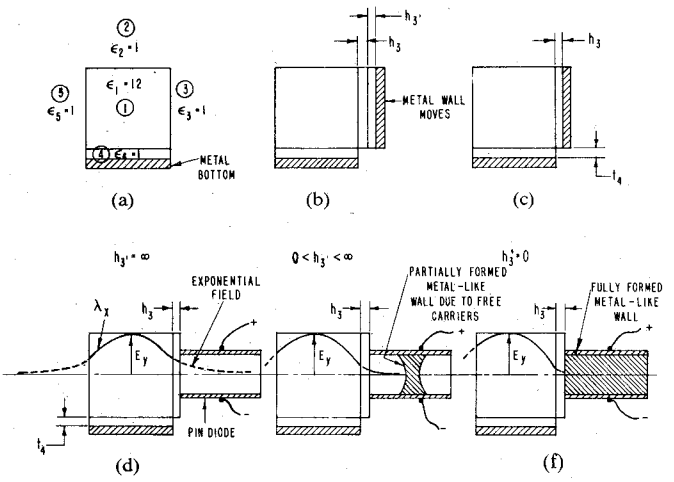

Fig. 2. Silicon waveguide, cross section, and *E*-field distribution. (a) Diodes unbiased (ideal), (b) diodes partially biased (ideal), (c) diodes fully biased (ideal), (d) field distribution diodes unbiased, (e) *E*-field distribution diodes small bias, (f) *E*-field distribution diodes fully biased.

Single-Frequency Electronic-Modulated Analog Line Scanning Using a Dielectric Antenna

R. E. HORN, SENIOR MEMBER, IEEE, H. JACOBS, FELLOW, IEEE, K. L. KLOHN, MEMBER, IEEE, AND E. FREIBERGS, MEMBER, IEEE

***Abstract*—A line scanning antenna is described whereby means of periodic perturbations and conductivity changes in p-i-n diode modulators, analog angular shifts of 5° can be obtained. The system is electronically modulated with relatively small power requirements.**

I. INTRODUCTION

In a recent report [1], an electronic modulated beam-steerable silicon waveguide array antenna was described. The construction of this device is shown in Fig. 1. It consisted of a silicon dielectric waveguide (runner), the ends of which were inserted into a metal waveguide and operated in the region of 60 to 70 GHz. The overall circuit arrangement was also described in the above referenced report. The basic concept for the operation of this device is as follows. As the energy propagates down the dielectric runner, an evanescent portion of the wave is in the air space surrounding the dielectric (Fig. 2) both in the vertical and horizontal directions. The perturbations on the top surface (copper strips) transform propagated energy to radiation. At any given frequency, the angle of radiation is a function of the guide wavelength λ_z and the perturbation spacing d. In this arrangement, d is fixed but the guide wavelength can be modified by the p-i-n diode modulators attached to the runner side wall. If the diodes are unbiased the wave will continue propagating down the runner with a guide wavelength λ_z. When the diodes are biased in the forward direction, they become conductive and act as if a conductive wall were placed on the runner sidewall (Fig. 2). This results in a new guide wavelength λ_z'. The result of the change in wavelength is that the radiation angle θ is changed, thus giving a line scan. The problem here is that the line scan is digital. There is a loss which occurs with an increase in the current in the modulating p-i-n diodes from 0 level to higher bias currents. This was shown in [1], where with zero bias an expected radiation pattern is obtained. With 300 mA (100 mA per diode) the pattern is shifted, $\Delta\theta = 9.5°$, but at intermediate currents, the radiation pattern deteriorated (i.e., attenuated and broadened). This behavior can be explained by realizing absorption of energy by the p-i-n diode modulators occurs when the diode current is low, since the conductivity of the intrinsic (I) region is intermediate between an insulator and a metallike conductor. In the intermediate conductivity state, the energy is not only being absorbed but is refracting into the lossy intrinsic medium. The fields in the runner and p-i-n modulator are envisaged as shown

Manuscript received September 4, 1981; revised November 23, 1981.

The authors are with the U.S. Army Electronics Technology and Devices Laboratory, Fort Monmouth, NJ 07703.

in Fig. 2. In Fig. 2(a), (b), and (c), a metal wall is brought in from infinity to a fixed position h_3, determined by a low permittivity spacer which will later also serve as a decoupling device to prevent the wave from diffracting entirely into the modulators. The presence of the metal wall has been found to increase λ_z thus making the radiation angle θ shift to a more negative value. In Fig. 2(d), (e), and (f), it was theorized that by changing the excess carrier density in the p-i-n diode *i*-region, a moving conduction wall will have a similar effect to a moving metal wall. This will be further described in the next section.

II. Proposed Experiment

In an attempt to minimize the absorption-refraction losses, the following experiment was tried. It was found necessary to use an optimum thickness (h_3) of low dielectric constant insulating layer between the silicon runner and the p-i-n diode modulators. The insulator serves as a spacer which provides less coupling from the runner to the long p-i-n diodes (total length is 2.4 cm) and hence little refraction into the diodes where losses occur due to absorption and reradiation. If the insulating layer is too thick there is less modulation, with the evanescent portion of the wave traveling down the runner undisturbed and little or no scan angle changes observed. The purpose of the following experiment was to determine an optimum thickness of insulation (h_3) to obtain a line scanning antenna which provides as nearly as possible a continuous analog scan.

In the experiment outlined in this paper, the moving wall concept is based on an increase of bias current with a resultant flooding of the entire diode from center outward (Fig. 2(e)). The reason for build-up carriers in the interior of the *I*-region is due to the presence of higher recombination rates at the surfaces and at the junction regions.

III. Experimental Data

The overall line scanning antenna structure as shown in Fig. 3 displayed results which will be of interest for specific applications. The dimensions of the runner were 11.0-cm overall length, 0.991-mm in width, and 1.01-mm in height. The perturbation spacing was 1.88 mm and the number of perturbation cells was 19. These cells were 0.5-mm wide and made of copper tape with an adhesive backing and attached directly to the silicon guide upper surface using the adhesive backing. The p-i-n diodes (1.2-cm long at the base, 1.1-cm long at the top, 1.0-mm high and 0.5-mm wide) were attached to the silicon guide sidewall using insulator tape with double sided adhesive (three tape layers). A copper layer was placed on the bottom of the runner with an insulator spacing (t_4) of 0.24 mm (three tape layers), the reason being that the radiation reflected upward gave approximately twice the radiated power when compared to no bottom reflection. The p-i-n modulators on the sidewall were separated from the silicon runners by 0.24 mm, a distance so far out that only a small part of the evanescent tail interacted with the diode modulators. This condition gave the best analog scanning results.

Experimental data as plotted in Figs. 4 through 6 show that analog scanning can be experimentally obtained over $\Delta\theta$ of about 5° with nearly uniform radiated power as a function of radiation angle.

In the experimental test (Figs. 4 and 5), the diode biasing current was increased in small increments and the estimated centroid of the radiation pattern was plotted in Fig. 6, together with the relative output power. The variation in radiated power was in the order of 2 dB or less over a $\Delta\theta$ variation of 5° at a frequency of 63.8 GHz.

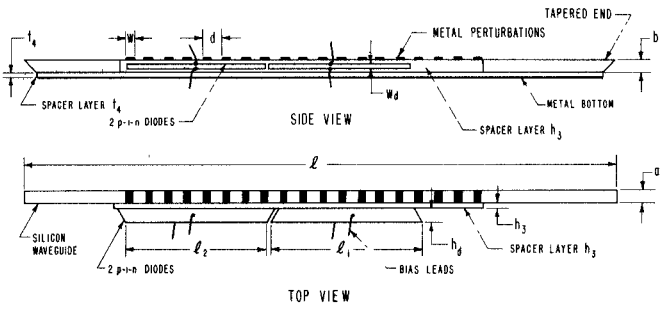

Fig. 3. Line scanning antenna, design parameters. n = numbers of metal perturbations = 19; a = dielectric waveguide width = 0.991 mm; b = dielectric waveguide height = 1.01 mm; d = perturbation spacing = 1.88 mm; t_4 = spacer layer thickness on bottom = 0.24 mm; l = dielectric waveguide length = 11.0 cm; h_3 = spacer layer thickness between waveguide and diodes = 0.24 mm. Diode length (l_1) = 1.2 cm; diode length (l_2) = 1.1 cm; diode height (h_d) = 1.0 mm; diode width (W_d) = 0.5 mm.

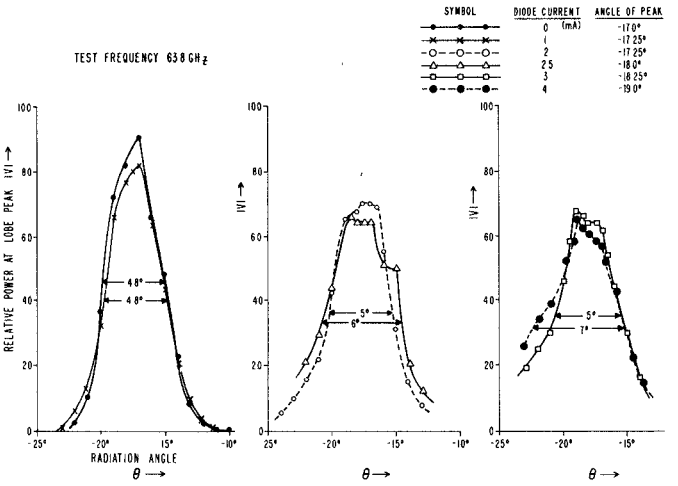

Fig. 4. Radiated power versus radiation angle as a function of bias current, (Part 1)

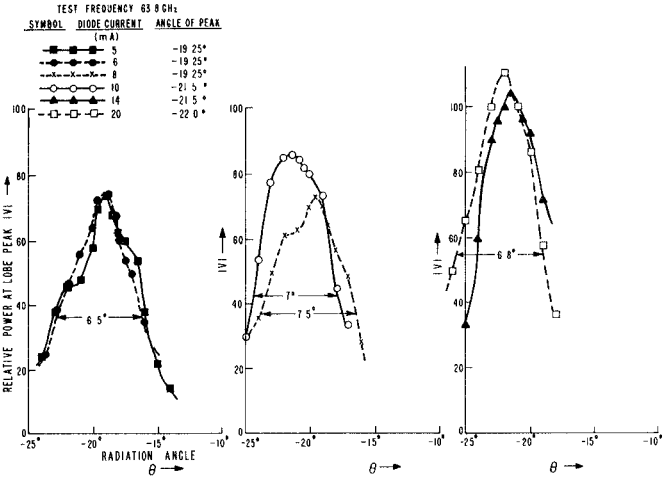

Fig. 5. Radiated power versus radiation angle as a function of bias current, (Part 2).

The test setup for this work used a 55 to 75-GHz source (square-wave modulated at 100° Hz) and a test fixture for metal-to-silicon guide transition. A pick-up horn was mounted in an angular calibrated arm directly over the perturbations at a dis-

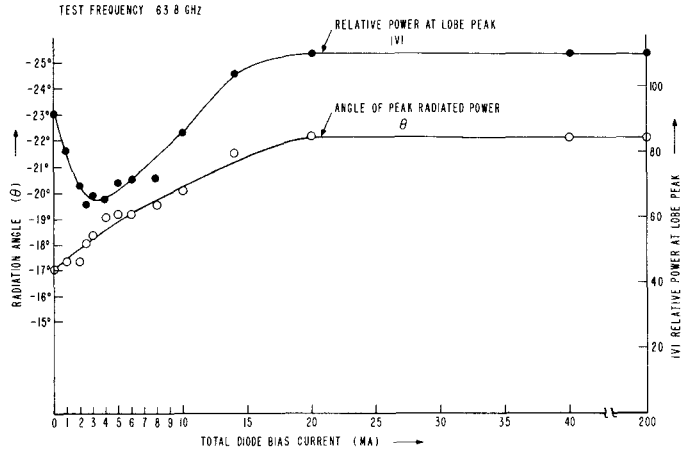

Fig. 6 Peak radiation angle and relative peak power versus bias current

TABLE I
PARAMETERS AND DEFINITIONS

SYMBOL	DESCRIPTION	DIMENSIONS
a	Silicon guide width	0.0991 cm
b	Silicon guide height	0.101 cm
fo	Frequency of source	63.8 GHz
λ_o	Wavelength of source	0.4702 cm
k	$2\pi/\lambda_o$ (Free space propagation constant)	13.363 cm^{-1}
ϵ_1	Silicon (Medium 1) relative dielectric constant	12
$\epsilon_{2,3,4,5}$	Air (Media 2,3,4,5)relative dielectric constant	1
h_5	Air dielectric thickness in medium 5	∞
h_3	Air dielectric thickness in medium 3	∞ or 0.024cm
t_2	Air dielectric thickness in medium 2	∞
t_4	Air dielectric thickness in medium 4	0.024 cm
m	Number of perturbations	19
d	Perturbation spacing (leading edge to leading edge)	0.188 cm
k_1	Propagation constant in silicon (medium 1)	46.290 cm^{-1}
q	Number of magnetic field extrema in the y dimension	1
$\xi_{3,5}$	Distance that the electric field penetrates the respective surrounding air medias 3 and 5 until the field has decayed to 1/e	0.02580 cm or .02612 cm
$\eta_{2,4}$	Distance that the magnetic field penetrates the respective surrounding air medias 2 and 4 until the field has decayed to 1/e	0.03007 cm
θ	Radiation angle referenced to normal (vertical from runner surface) (see Fig. 2)	-17.5^0 or -22^0
n	Spacial harmonic of radiation (Possible values 0, ± 1, ±2...)	-1
p	Number of electric field extrema in the x dimension	1

tance of 20 cm. The pick-up horn was terminated in a square-law diode detector for direct power measurements. This placed the detector in the far field region.

IV. Analysis

Equations (1) and (2) were derived by Jacobs and Schwering [2] for a dielectric waveguide surrounded by metal walls. Here, a is the width of the dielectric, b is the dielectric height, the distance from silicon dielectric to metal wall in the x direction is $h_{3,5}$, and $t_{2,4}$ is the distance to the metal wall in the y direction. In this case, (1) through (8) can be used to calculate λ_z and θ. The design parameters are listed in Table I. The design equations are as follows:

$$ak_x = p\pi - \tan^{-1}[k_x\xi_3 \tanh(h_3/\xi_3)] - \tan^{-1}[k_x\xi_5 \tanh(h_5/\xi_5)] \quad (1)$$

TABLE II
THEORETICAL AND EXPERIMENTAL RESULTS AT 63.8 GHz

CONFIGURATION	k_x cm^{-1}	k_y cm^{-1}	k_z cm^{-1}	$\xi_{3,5}$ cm	$\eta_{2,4}$ cm	CALCULATED λ_z cm	CALCULATED θ cm	EXPERIMENTAL θ
A. Diodes Non Conducting	21.485	29.288	28.6946	0.02580	0.03007	0.21897	-20.72°	-17.0°
B. Diodes Fully-Conducting	22.333	29.288	28.0395	0.02612	0.03007	0.22408	-23.75°	-22.0°

and

$$bk_y = q\pi - \tan^{-1}\left[\frac{\epsilon_2}{\epsilon_1} k_y \eta_2 \coth(t_2/\eta_2)\right] - \tan^{-1}\left[\frac{\epsilon_4}{\epsilon_1} k_y \eta_4 \coth(t_4/\eta_4)\right] \quad (2)$$

where

$$k_z = \sqrt{k_1^2 - k_x^2 - k_y^2} \quad (3)$$

and

$$\eta_{2,4} = \left[\left(\frac{\pi}{A_{2,4}}\right)^2 - k_y^2\right]^{-1/2} = \frac{1}{k_{y_{2,4}}} \quad (4)$$

$$\xi_{3,5} = \left[\left(\frac{\pi}{A_{3,5}}\right)^2 - k_x^2\right]^{-1/2} = \frac{1}{k_{x_{3,5}}} \quad (5)$$

$$A_{2,3,4,5} = \frac{\lambda_0}{2\sqrt{\epsilon_1 - \epsilon_{2,3,4,5}}}. \quad (6)$$

As k_x or k_y changes, the guide wavelength also changes since

$$\lambda_g = \lambda_z = 2\pi/k_z. \quad (7)$$

This change in λ_z will, in turn, cause a shift in the angle of radiation as derived by Oliner [3] as follows:

$$\theta_n = \sin^{-1}\left(\frac{\lambda_0}{\lambda_g} + \frac{n\lambda_0}{d}\right), \qquad n = -1 \quad (8)$$

where

$$\left|\frac{\lambda_0}{\lambda_g} + \frac{\lambda_0}{d} n\right| \leq 1.$$

In the limiting case, when the metal walls are infinitely far away from the dielectric waveguide ($h_{3,5}$ and $t_{2,4} = \infty$), (1) and (2) reduce to the equations for no metal walls as follows:

$$ak_x = p\pi - \tan^{-1}[k_x \xi_3] - \tan^{-1}[k_x \xi_5] \quad (9)$$

$$bk_y = q\pi - \tan^{-1}\left[\frac{\epsilon_2}{\epsilon_1} k_y \eta_2\right] - \tan^{-1}\left[\frac{\epsilon_4}{\epsilon_1} ky \eta_4\right] \quad (10)$$

since $\tanh(x)$ and $\coth(x)$ both approach one as x approaches infinity. These are the equations developed by Marcatili [4]. Equation (9) applies for unbiased diodes. Equation (10) however does not since a metal layer is at a distance t_4 from the runner bottom so that the last term of (10) is modified as shown in the last term of (2).

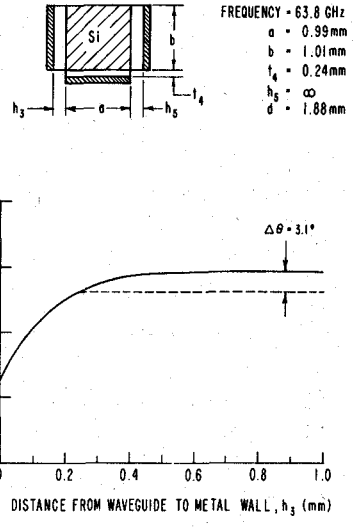

Fig. 7. Radiation angle versus diode distance, calculated.

To verify experimental results, a series of calculations were made using (1) through (6), plotted in Fig. 7 and zero and maximum current limits tabulated in Table II. Fig. 7 shows the condition where two side walls have been moved to infinity and the metal wall on the bottom is 0.24 mm. This figure shows the effects on θ_n as the right side metal wall is moved in from ∞ to 0. The limits of the calculated angular shift $\Delta\theta$ is 17°. Experimentally, however, the wall is moved from ∞ to only 0.24 mm with a resultant angular shift of $\Delta\theta = 3.5°$, which is in close agreement with the experimental results of $\Delta\theta \approx 5°$.

Practical limitations of power losses (outlined above) experimentally limit the side wall spacing h_3 to a minimum thickness of 0.24 mm with a resultant measured angular shift, $\Delta\theta = 5.0°$. If $h_3 \ll 0.24$ mm, attenuation losses and beam broadening occur which mask the analog processes.

V. APPLICATIONS

A new type of line scanner is described in which analog scanning can be obtained. The angle of scan was found to be 5°. The operation was at a single frequency and the scanning was electronic with relatively small power requirements (1 V×50 mA per diode). Such a device may be useful in communications where a small amount of scanning is needed to locate other communicators. Another application might be for small missiles or projectiles where these angles of scan are required for target tracking with millimeter wave radiation.

VI. Conclusion

We note in the theoretical calculations that $\Delta\theta = 3.5°$ was obtained which is reasonably close to the experimental measurements of $\Delta\theta \approx 5.0°$. We conclude that (1) and (2) are valid approximations. A further conclusion is that for large insulator spacing between the runner and p-i-n diode modulator and with the diode unbiased, only a small edge of the evanescent wave interacts with the p-i-n modulator. Since the coupling is small, the wave is relatively undisturbed. With full forward bias applied to the p-i-n diode, a conductive wall forms and changes the transmitted wavelength. Due to the relatively thick insulator layer, the interaction is so small that refraction does not significantly occur although a slight amount of absorption still results. In this condition, a small amount of angular scan can occur and with low attenuation and negligible beam spreading. This is verified by analysis of the experimental data which shows that as the forward bias current is increased in small increments, the radiated beam starts to shift with some attenuation. As the current is increased to 50 mA and above, the angular shift increases to its maximum value and the attenuation is reduced to almost zero as it was with zero bias current. It should be noted that the analog effect starts to occur for low current levels of 1 mA. Above 50 mA, no further effect is observed. This indicates that diodes become conductive at very low-current levels and reach a maximum conducting level at less than 25 mA per diode.

Acknowledgment

The authors wish to acknowledge help from Dr. F. Schwering for consultation on the analysis and to E. Malecki for construction of the p-i-n diodes.

References

[1] R E Horn, H. Jacobs, E Freibergs, and K. L. Klohn, "Electronic modulated beam-steerable silicon waveguide array antenna," *IEEE Trans. Microwave Theory Tech.*, vol. MTT-28, pp 647–653, June 1980.
[2] H. Jacobs and F. K. Schwering, private communication
[3] A. A. Oliner, Polytechnic Institute of New York, private communication.
[4] E. A. J. Marcatili, "Dielectric rectangular waveguide and directional coupler for integrated optics," *Bell Syst. Tech. J.*, vol. 48, no 7, Sept 1969.

Diffraction Loss in Dielectric-Filled Fabry–Perot Interferometers

PAUL F. GOLDSMITH, MEMBER, IEEE

Abstract—**We analyze the transmission of dielectric-filled Fabry–Perot interferometers excited by a spherical wave having a Gaussian amplitude distribution transverse to the axis of propagation. The loss due to diffraction experienced by the incident mode is found to be reduced by a factor $\geq n^4$ when n, the index of refraction of the dielectric, is significantly greater than unity, thus permitting such devices to be used with low loss in beams of considerably greater angular divergence than possible with air-filled interferometers. Measurements at 3-mm wavelength of devices made of quartz and sapphire are presented, which are in good agreement with the theoretical calculations.**

Manuscript received October 19, 1981; revised December 1, 1981 This work was supported in part by the National Science Foundation under Grant AST 80-26702 This is contribution Number 499 of the Five College Observatory.

The author is with the Five College Radio Astronomy Observatory, 619 Graduate Research Center, University of Massachusetts, Amherst, MA 01003.

I. Introduction

Fabry–Perot interferometers have been employed at millimeter wavelengths as single-sideband filters [1], [2], and as local oscillator injectors [2], [3]; the primary incentive for their use is the lower loss obtainable with quasi-optical devices compared to their waveguide analogs used at lower frequencies. In order to achieve a high level of performance, the effects of diffraction must be considered; these impose a lower limit to the beam diameter that can be employed. The effects of diffraction on Fabry–Perot interferometer performance at microwave frequencies have been treated in considerable detail by Arnaud, Saleh, and Ruscio [4] (hereafter ASR). These authors treat the diffraction loss at normal incidence, as well as the additional walk-off loss that occurs at oblique incidence. In the present work, we extend their formulation to explicitly include dielectric-filled interferometers, and present some design curves for calculating the transmission of the fundamental mode under excitation by a gaussian beam.

II. Fabry–Perot Interferometer

A. Geometrical Optics Limit

The Fabry–Perot interferometer is considered to consist of two infinite plane mirrors, each having power reflectivity $R = |\rho e^{i\phi_r}|^2$, where ρ is the amplitude, and ϕ_r the phase of the electric field reflection coefficient. The mirrors are considered to be lossless, that is, $R = 1 - T$, where T is the power transmission coefficient. We define $T = |te^{i\phi_t}|^2$, t, and ϕ_t being the magnitude and phase of the field transmission. In the absence of diffraction (plane wave or geometrical optics limit) the fraction of incident power transmission is given by [5]

$$|\tau|^2 = \frac{\xi^2\left(\frac{1-R}{1-\xi^2 R}\right)^2}{1+\frac{4\xi^2 R}{(1-\xi^2 R)^2}\sin^2(\delta\phi/2)} \tag{1}$$

where ξ^2 is the one-way power transmission of the medium between the mirrors, and $\delta\phi$ is the round-trip phase delay. The round-trip phase delay is

$$\delta\phi = 2\phi_r + (4\pi d/\lambda)(n^2 - \sin^2 i)^{1/2} \tag{2}$$

for an interferometer with mirror spacing d, a medium between the mirrors having index of refraction n, and with the direction of the incident radiation being at an angle i from normal incidence. For an interferometer consisting only of a slab of dielectric, the power reflection coefficient at each interface is obtained from the Fresnel equations [6], and $2\phi_r = 2\pi$. For mirrors consisting of metallic mesh, for example, the reflection coefficient and phase are more complicated and generally quite frequency-dependent [7].

B. Gaussian Beam Excitation

Many types of microwave feedhorns as well as beam-waveguide systems produce radiation patterns which can be reasona-

0018-9480/82/0500-0820$00.75 ©1982 IEEE